

Absolute Amplitude and Growth Time of Electron Plasma Waves Excited by Two Laser Beams

Behrouz Amini

University of California, Los Angeles, California 90024

(Received 21 November 1984)

Excitation of electron plasma waves in a hot and fully ionized plasma by two laser beams is presented. The growth time and absolute amplitude of the excited waves, measured by light scattering, indicate very strong coupling of the laser light with the plasma.

PACS numbers: 52.35.Mw, 42.65.Cq, 52.25.Rv, 52.50.Gj

Nonlinear excitation of plasma waves by two electromagnetic beams has been of great interest as a result of its applications in plasma physics. Of particular importance is the possibility of using this mechanism to heat the laboratory fusion devices by presently available high-power laser or rf beams. Some other applications besides plasma heating¹⁻³ are plasma diagnostics,⁴⁻⁶ studying and controlling ionospheric plasmas,⁷ and, as shown here, studies of filamentation.

A number of theorists have investigated the excitation of plasma waves by two laser beams. Among them Rosenbluth and Liu calculated the saturation amplitude of a cold plasma involving relativistic effects. Lee *et al.*⁸ predicted a smaller value by including collisional damping. Schmidt⁹ employed kinetic descriptions in a hot plasma. Experimentally, there have been only two observations confirming the density resonance.^{10,11}

In this Letter, the growth time and absolute amplitude of the excited electrostatic waves are presented. From these fundamental quantities, the strength of the coupling of the laser with the plasma and, as a result, the efficiency of "beat heating" are tested.

The experimental arrangement has been reported previously.¹¹ Two counterpropagating CO₂ laser beams at 10.3- and 9.6- μ m wavelength with finite bandwidth and full width at half maximum of 50 nsec were used to excite the plasma wave at the difference frequency, and a third beam from a ruby laser was used to detect the plasma wave by Thomson scattering. The helium plasma which was produced in a fast theta pinch was fully ionized with $T_e \approx 30$ eV and $T_i \approx 80$ eV. The electron density for excitation was around 4.8×10^{16} cm⁻³ and as a result of the finite spectral width of the pump there was a range of density for resonance.

In the experiment to be described, the design and parameters are carefully chosen so as to eliminate possible ambiguities in the interpretation of data. Among these are the following: (1) The driving beams overlap coaxially and at the center of the plasma column the spot sizes are 1.7×2.5 and 2.5×3.5 mm², therefore assuring a large overlap of 1.7×2.5 mm². The ruby light is then focused to a smaller spot size in the interaction region defined by the overlap of the CO₂

beams. As a result, the interaction length along the ruby light L_0 is well defined ($L_0 \approx 2.5$ mm). (2) The average intensities of the pump beams are kept below the stimulated Raman instability threshold observed previously in this plasma. (3) The plasma is hot and fully ionized. As a result, the temperature increase due to inverse bremsstrahlung absorption is negligible. Experimentally there is no measurable increase in the intensity of the normal satellite caused by either of the pump beams. (The word "normal satellite" is used for the electron satellite without the pump beam.) Recall that $\int S(k, \omega) d\omega \approx 1/\alpha^2$, where $S(k, \omega)$ is the spectral density function and $\alpha = 1/k\lambda_D$ is the correlation parameter. Therefore the intensity of the normal satellite scales with the temperature.

Time and space variations of plasma density are measured independently by simultaneous end-on (along the plasma column) and side-on (across the plasma column) holographic interferometry¹² in conjunction with the signal from a photodiode monitoring the plasma radiation. The side-on hologram also gave directly the density scale length along the axis in the central region. In this experiment the radiation from the interaction region is used to monitor the plasma density variations in time. This radiation scales with the square of the electron density and is, therefore, very sensitive to plasma density.

Figures 1 and 2 show a typical normal satellite, and the scattered light from the excited plasma wave, respectively, on a 2-m 500-channel spectrograph. The

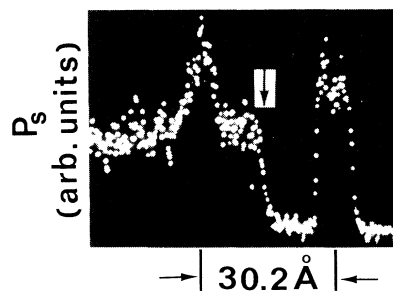


FIG. 1. Normal satellite on the left and the unshifted stray light on the right. The portion to the right of the arrow has been attenuated to show the unshifted light.

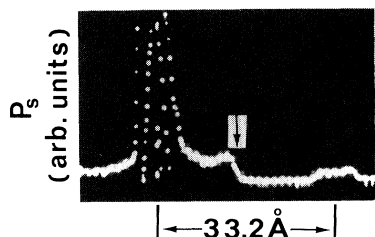


FIG. 2. Scattered spectrum from the excited plasma wave on a reduced vertical scale. (The reduction factor can be visualized from the unshifted light by comparing this and Fig. 1.) This is a single peak which is broken symmetrically, by instrument, into five pieces in order to be displayed on the screen.

dispersion on the spectrograph is 0.2 \AA per channel and each dot represents a channel. In both Figs. 1 and 2 the plasma density at the center is relatively constant during the 25-nsec duration of the diagnostic beam. The equation relating the plasma wave amplitude \tilde{n}/n_0 to the ratio of the scattered to incident light power p_s/p_0 is given by¹³

$$\tilde{n}/n_0 = 2(p_s/p_0)^{1/2}/r_0\lambda_0n_0L, \quad (1)$$

where r_0 is the classical radius of the electron, λ_0 is the wavelength of the diagnostic beam, and L is the size of the resonant region along the diagnostic beam. For the normal satellite $L \approx 5.5 \text{ mm}$, which is the extent of uniform density at the center of the plasma column,^{11,12} and the measured value of p_s/p_0 is 2.3×10^{-12} .

To find L for the scattered light we inspect the interaction region. Outside the CO_2 -laser oscillator a grating was used to split the pump beams. The two beams centered at 9.56 and 10.27 \mu m each have four dominant lines with a total frequency spread of $(\Delta\omega/\omega)_{1,2} \approx 1.1 \times 10^{-2}$. By combination of a lens and the grating, the frequency of each beam along the 2.5-mm interaction region L_0 , which is away from the focal spot, changes steadily from one end to the other. This frequency change along L_0 was set up to be increasing for one beam while decreasing for the other beam, thus producing a large difference frequency along L_0 . For the plasma wave which grows at the difference frequency this gives

$$\Delta\omega/\omega \approx (\Delta\omega_1 + \frac{5}{7}\Delta\omega_2)/(\omega_1 - \omega_2)$$

and

$$\Delta k/k \approx (-\Delta k_1 + \frac{5}{7}\Delta k_2)/(k_1 + k_2).$$

The factor $\frac{5}{7}$ is from the geometry. Here, $\Delta\omega$ corresponds to about 45 channels. Since the plasma is uniform at the interaction region^{11,12} and the difference frequency of the driving beams at a given point along L_0 is constant with time, for those shots where the

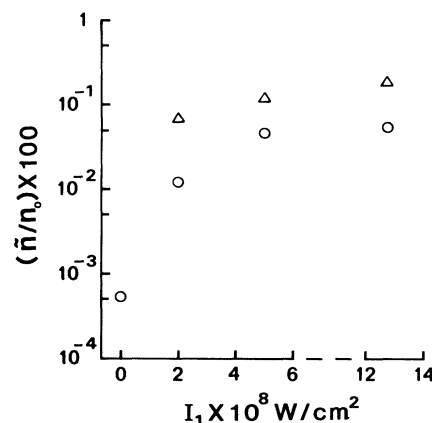


FIG. 3. The measured amplitude of the plasma wave vs the intensity of the $9.6\text{-}\mu\text{m}$ beam is shown by open circles. The experimental variation of the first point, obtained from the normal satellite, is $\pm 3\%$ and for the last three points is $\pm 12\%$. The predicted values are indicated by triangles.

plasma frequency matches the difference frequency the perfect matching occurs in a small region (ideally, at one point) and so the resonant region L will be limited by the frequency mismatch introduced by the pump beams. By including a 12-channel instrumental width, we find from Fig. 2 that the contribution of L to the width is 13 channels. This will give $L \approx 0.5 \text{ mm}$ (see below).

The measured absolute amplitude, calculated from Eq. (1), as a function of the $9.6\text{-}\mu\text{m}$ beam intensity I_1 , is shown with open circles in Fig. 3. On this plot the intensity of the $10.3\text{-}\mu\text{m}$ beam, $I_2 \approx 1.3 \times 10^8 \text{ W/cm}^2$, is constant. The first point indicates the initial fluctuation level obtained from the normal satellite.

To measure the growth time, the timing was set so that during the 25-nsec duration of the ruby light, the plasma density at the interaction region had the steepest change in time. This rapid change of plasma density occurs during the wave breaking of a macroscopic instability¹² combined with decreasing magnetic field of the theta pinch between the two half cycles. Consequently, in these shots the resonant region L is swept through the interaction length L_0 in less time than 25 nsec. The result is demonstrated in Fig. 4. From the plasma time monitor and ruby light timing, the sweep time is expected to be about 10 nsec. Fifty-nine channels responded to the scattered light in Fig. 4. Therefore, on the average, each channel is exposed to the peak of the scattered light for about $\frac{10}{59} = 0.17$ nsec. (This time will be longer if one includes the width of the ruby light.) During this time, the amplitude of the plasma wave, from this and similar shots, increases about 50–55 times above the initial fluctuation. This value which is the average value during this short period of time is only less than 40% smaller than

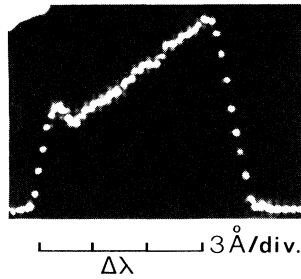


FIG. 4. Scattered spectrum during the time that the plasma density had the steepest change. The width of the scattered light indicates the bandwidth of the driving beams.

the average value obtained in shots like Fig. 2. Now let us view the problem in terms of mapping. In each shot the scattered light maps the resonant region into certain channels on the spectrograph. The entire interaction region L_0 can be mapped either with different shots by different plasma density or, as in Fig. 4, in a single shot with rapid change of density. The resonant region $L \approx 0.5$ mm referred to previously was obtained by multiplication of L_0 by $\frac{13}{59}$, where 13 and 59 are the number of channels which L and L_0 have been mapped into, respectively. It is worthwhile to mention that by masking portion(s) of the $9.6\text{-}\mu\text{m}$ beam it was proven, as one expects from the setup, that this mapping is single valued.

Figure 5 shows a sample picture with the timing similar to Fig. 4. The portion of the scattered light which is missing in Fig. 5, but is filled in for the same channels in Fig. 4, is possibly due to filamentation. Detailed study of filamentation is possible by simply imaging the interaction region onto a two-dimensional array detector, like a CCD (charge-coupled device).

The contribution of the relativistic effects in the saturation of the plasma wave amplitude is due to a frequency mismatch of the order of $(v^2/c^2)\omega_p$, where v is the longitudinal quiver velocity of the electron. Since $v = (\tilde{n}/n_0)v_{ph}$, where v_{ph} is the phase velocity, and in this experiment $v_{ph}/c = 0.035 \ll 1$, the relativistic effects are negligible. However, the saturation and the growth of the plasma wave due to damping rate γ_L , under the assumption that $\gamma_L \ll \omega$, is given by

$$\tilde{n}/n_0 = (v_1 v_2 \omega / 4 v_{ph}^2 \gamma_L) (1 - e^{-\gamma_L t}), \quad (2)$$

where $v_i = eE_j/m\omega_j$ are the transverse quiver velocities. This equation was obtained by inclusion of the damping in Ref. 1 and the use of the Green's function to solve the differential equation. For $\gamma_L t \gg 1$, Eq. (2) reduces to the asymptotic value calculated by Schmidt. The inhomogeneity of plasma along the driving beams which was not considered in Eq. (2) is not significant. As was shown earlier,¹⁴ for a given density scale length the interaction length along the driving beams L_D (the size of the region where the

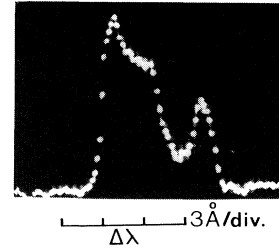


FIG. 5. The valley in the scattered light spectrum is possibly due to filamentation of the driving beams.

three waves phase lock) is larger for a symmetrical density profile than a linear one. In this experiment, because of the parabolic profile, the growth time is much smaller than L_D/v_g , where v_g is the group velocity. As a result, the plasma can be considered homogeneous. Moreover, dissipation of energy by damping dominates the convection, that is, $\gamma_L E^2/8\pi \gg (v_g/L_D) E^2/8\pi$.

Numerically, $\gamma_L \approx 4 \times 10^{10}$; then the growth time of the plasma wave to reach the saturation level is expected to be around 0.1 nsec. The measured value, demonstrated in Fig. 4, is an upper limit and agrees with Eq. (2). Note that during saturation, collisions ($\gamma_c \approx 5 \times 10^9$) might help dissipation by Landau damping to maintain its dominance.¹⁵

The predicted amplitude obtained from Eq. (2) is shown by triangles in Fig. 3. Although the disagreement between the measured and predicted values is small, except at the second point, these lower experimental values were expected. This is due to depletion of the pump beams combined with the long plasma column, since the plasma wave can grow at either side of the plasma column, while the diagnostic beam only scans the central region. Finally, in Fig. 3, the measured values of the last two points are at nearly the same level. (Note that the ion dynamics, which can saturate the plasma wave,¹⁶ is negligible as a result of the weak longitudinal field.) One possible reason for this is depletion of beam 2 (the weaker beam). Experimentally, this statement is supported by the fact that the scattered light level decreases by attenuation of the second beam at the last point of Fig. 3. From the discussion of this paragraph one can conclude with some assurance that beat heating can be used to heat fusion devices efficiently, although the maximum heating efficiency is limited to ω/ω_1 .²

In conclusion, the growth time and absolute amplitude of the plasma waves, excited by optical mixing of two laser beams, have been measured. The measured values are in reasonable agreement with theory. It was also shown that optical mixing can be used to study filamentation directly, and that the laser light couples very strongly with the plasma, so that beat heating is suitable for heating plasmas.

I am grateful to G. J. Morales, R. L. Stenzel, E. M.

Campbell, and C. A. Whitten for the useful comments and support. This work was supported in part by the Lawrence Livermore National Laboratory, Order No. 3446905.

¹M. N. Rosenbluth and C. S. Liu, Phys. Rev. Lett. **29**, 701 (1972).

²B. Cohen, A. N. Kaufman, and M. Watson, Phys. Rev. Lett. **29**, 581 (1972); A. N. Kaufman and B. Cohen, Phys. Rev. Lett. **30**, 1306 (1973); B. Cohen *et al.*, Phys. Fluids **18**, 470 (1975).

³V. Fuchs *et al.*, Phys. Rev. Lett. **31**, 1110 (1973).

⁴N. Kroll, A. Ron, and N. Rostoker, Phys. Rev. Lett. **13**, 83 (1964).

⁵R. Cano, I. Fidone, and B. Zarfagna, Phys. Fluids **14**,

811 (1971).

⁶E. S. Weibel, Phys. Rev. Lett. **37**, 1619 (1976).

⁷G. Weyl, Phys. Fluids **13**, 1802 (1970).

⁸P. S. Lee *et al.*, Phys. Rev. Lett. **30**, 538 (1973).

⁹G. Schmidt, Phys. Fluids **16**, 1676 (1973).

¹⁰B. L. Stansfield, R. Nodwell, and J. Meyer, Phys. Rev. Lett. **26**, 1219 (1971).

¹¹B. Amini *et al.*, Phys. Rev. Lett. **53**, 1441 (1984).

¹²B. Amini, Phys. Fluids **28**, 387 (1985).

¹³See, for example, R. E. Slusher *et al.* Phys. Fluids **23**, 472 (1980).

¹⁴B. Amini *et al.*, University of California, Los Angeles Report No. UCLA PPG-746, 1983 (unpublished); F. S. Chen *et al.*, in Proceedings of the International Conference on Plasma Physics, Lausanne, Switzerland, 27 June–3 July 1984 (to be published).

¹⁵J. S. DeGroot, private communication.

¹⁶T. W. Johnston, private communication.